ON THE SIMULATION OF AERODYNAMIC NOISE WITH DIFFERENT TURBULENCE MODELS

X. Huang[1,2], M. Schäfer[1,2]

[1]Graduate School Computational Engineering
Technische Universität Darmstadt
Dolivostrasse 15, 64293 Darmstadt, Germany
{huang, schaefer}@gsc.tu-darmstadt.de

[2] Institute of Numerical Methods in Mechanical Engineering
Technische Universität Darmstadt
Dolivostrasse 15, 64293 Darmstadt, Germany
{huang, schaefer}@fnb.tu-darmstadt.de

Keywords: Aeroacoustics, Turbulence Model, LEE.

Abstract. *This paper investigates the performance of different turbulence models for simulating the aeroacoustic field generated by turbulent flow. The acoustic field is calculated by solving the linearized Euler equations (LEE), while the acoustic source is obtained by solving the incompressible Navier-Stokes equations. Three different turbulence models are adopted for the flow simulation: the large eddy simulation (LES), the delayed detached-eddy simulation (DDES) and unsteady Reynolds Averaged Navier-Stokes equations (URANS). The acoustic sources are calculated on a flow grid and then transferred and interpolated onto an acoustic grid, enabling the acoustic computation of the far field with a reasonable computational cost. We present the acoustic sources calculated using different turbulence models. Furthermore, we compare the sound pressure level (SPL) spectra of different turbulence models with the experimental data.*

1 INTRODUCTION

In recent decades, the simulation of aerodynamic noise has become increasingly significant for engineering applications. The prediction of aeroacoustic fields can be realized using the direct noise computation (DNC) [1], which solves the compressible Navier-Stokes equations directly for flow and acoustics. However, due to the significant difference at both length and time scales of flow and acoustic fields, the DNC method is considered inefficient especially for low Mach number flows. A hybrid scheme is commonly adopted, in which the simulations of flow and acoustics are separated and coupled through the acoustic sources.

Regarding the simulation of acoustics, several integral formulations, such as Lighthill's analogy [8, 9] and Curle's analogy [2] have been successfully applied. An alternative is the linearized Euler equations (LEE) method, which is obtained by using the Expansion about Incompressible Flow (EIF) technique [12, 13].

In order to acquire the acoustic sources, the incompressible Navier-Stokes equations are utilized. For turbulent flows, direct numerical simulation (DNS) in most cases cannot be applied due to its unaffordable computational cost. A turbulence model is usually adopted to characterize the unresolved turbulence scales, leading to a significant reduction in computational cost. Large eddy simulation (LES) resolves the large eddies and implicitly accounts for the small eddies by using a sub-grid scale model. Nevertheless, the computational cost of LES for engineering problems is mostly beyond the current computational power. Reynolds Averaged Navier-Stokes (RANS) equations only resolve the time averaged flow, leading to a drastic reduction of computational cost. However, the lack of accuracy makes it inappropriate for aeroacoustic problems. By adding an additional unsteady term to the RANS equations, one obtains the unsteady RANS (URANS) model. The idea of hybrid methods is to combine the advantages of LES model and RANS models. Detached-eddy simulation (DES) is one of the most popular hybrid turbulence models. The DES model switches between LES and RANS modes according to the numerical resolution [15, 16].

In the present work, the results of three turbulence models are compared with the experimental data to determine their suitability in the prediction of aerodynamic noise.

2 GOVERNING EQUATIONS

2.1 Linearized Euler equations for aeroacoustic simulation

The acoustic field is described through three quantities: the acoustic pressure p^{ac}, the acoustic density fluctuation ρ^{ac} and the particle velocity u_i^{ac}. These are the perturbation of pressure, density and velocity caused by sound waves, respectively. Since the humans' sensation of sound is proportional to the logarithm of the acoustic pressure, the acoustic pressure is rarely used in practice. The sound pressure level (SPL) L_p with unit decibel (dB) is commonly adopted, which is defined by

$$L_p = 10 \cdot \lg \frac{\left(p_{\text{eff}}^{\text{ac}}\right)^2}{p_{\text{ref}}^2} = 20 \cdot \lg \frac{p_{\text{eff}}^{\text{ac}}}{p_{\text{ref}}}, \tag{1}$$

where p_{ref} is a reference acoustic pressure and $p_{\text{eff}}^{\text{ac}}$ is the effective acoustic pressure given by

$$p_{\text{eff}}^{\text{ac}} = \sqrt{\frac{1}{T} \int_{t=0}^{T} (p^{\text{ac}}(t))^2 \, \mathrm{d}t}. \tag{2}$$

In order to derive the governing equations for the acoustic quantities, a decomposition technique called Expansion about Incompressible Flow method (EIF) is utilized. This technique is

proposed by Hardin, Pope [6] and improved by Shen and Sørensen [12, 13]. It assumes that the compressible flow field at low Mach number can be decomposed into an incompressible flow field and an acoustic field

$$u_i = u_i^{\text{inc}} + u_i^{\text{ac}}, \tag{3}$$

$$p_i = p_i^{\text{inc}} + p_i^{\text{ac}}, \tag{4}$$

$$\rho_i = \rho_i^{\text{inc}} + \rho_i^{\text{ac}}, \tag{5}$$

where u_i, p_i and ρ_i are the velocity, pressure and density of compressible flow and superscripts inc and ac represent the components of incompressible flow and acoustic field respectively. Based on the EIF decomposition, one can obtain the linearized Euler equations (LEE) as follows

$$\frac{\partial \rho^{\text{ac}}}{\partial t} + \rho^{\text{inc}} \frac{\partial u_i^{\text{ac}}}{\partial x_i} + u_i^{\text{inc}} \frac{\partial \rho^{\text{ac}}}{\partial x_i} = 0, \tag{6}$$

$$\rho^{\text{inc}} \frac{\partial u_i^{\text{ac}}}{\partial t} + \rho^{\text{inc}} u_j^{\text{inc}} \frac{\partial u_i^{\text{ac}}}{\partial x_j} + \frac{\partial p^{\text{ac}}}{\partial x_i} = 0, \tag{7}$$

$$\frac{\partial p^{\text{ac}}}{\partial t} + c^2 \rho^{\text{inc}} \frac{\partial u_i^{\text{ac}}}{\partial x_i} + c^2 u_i^{\text{inc}} \frac{\partial \rho^{\text{ac}}}{\partial x_i} = -\frac{\partial p^{\text{inc}}}{\partial t}. \tag{8}$$

For more details regarding the derivation of the above equations, the reader is referred to [7].

2.2 Turbulent flow

For turbulent flows, the governing equations read

$$\frac{\partial \overline{u_i^{\text{inc}}}}{\partial x_i} = 0, \tag{9}$$

$$\frac{\partial \overline{u_i^{\text{inc}}}}{\partial t} + \overline{u_j^{\text{inc}}} \frac{\partial \overline{u_i^{\text{inc}}}}{\partial x_j} = \frac{\partial}{\partial x_j} \left(\nu \frac{\partial \overline{u_i^{\text{inc}}}}{\partial x_j} - \tau_{ij} \right) - \frac{1}{\rho^{\text{inc}}} \frac{\partial \overline{p^{\text{inc}}}}{\partial x_i}. \tag{10}$$

For URANS models, $\overline{u_i^{\text{inc}}}$ is the mean velocity, while for LES models $\overline{u_i^{\text{inc}}}$ is the filtered velocity. This similarity of the equations of URANS and LES facilitates the development of hybrid RANS/LES models [4].

$k - \omega$ **SST model**   For URANS models, τ_{ij} in (10) is the Reynold's stress, which is usually calculated using the Boussinesq approximation

$$\tau_{ij} = \nu_{\text{t}} \left(\frac{\partial \overline{u_i^{\text{inc}}}}{\partial x_j} + \frac{\partial \overline{u_j^{\text{inc}}}}{\partial x_i} \right) - \frac{2}{3} k \delta_{ij}, \tag{11}$$

where ν_{t} is the turbulent viscosity that has to be modeled. The $k - \omega$ SST model is a URANS model applying the $k - \omega$ model in the near wall region and the $k - \varepsilon$ model in the free stream region. Therefore, it combines the advantages of both basic URANS models [10]. The $k - \omega$ SST model is formulated as

$$\frac{\partial k}{\partial t} + \overline{u_j^{\text{inc}}} \frac{\partial k}{\partial x_j} = P_k - \beta^* k \omega + \frac{\partial}{\partial x_j} \left[(\nu + \sigma_k \nu_t) \frac{\partial k}{\partial x_j} \right], \tag{12}$$

$$\frac{\partial \omega}{\partial t} + \overline{u_j^{\text{inc}}} \frac{\partial \omega}{\partial x_j} = \frac{\gamma}{\nu_t} P_k - \beta \omega^2 + \frac{\partial}{\partial x_j} \left[(\nu + \sigma_\omega \nu_t) \frac{\partial \omega}{\partial x_j} \right] + 2(1 - F_1) \frac{\sigma_{\omega 2}}{\omega} \frac{\partial k}{\partial x_j} \frac{\partial \omega}{\partial x_j}, \tag{13}$$

where k is the turbulent kinetic energy, ω is a specific dissipation, P_k is the production term given as

$$P_k = \tau_{ij} \frac{\partial \overline{u_i^{\text{inc}}}}{\partial x_j}. \tag{14}$$

The turbulent viscosity is calculated using

$$\nu_t = \frac{a_1 k}{\max(a_1 \omega, \Omega F_2)}, \tag{15}$$

where Ω is the vorticity magnitude

$$\Omega = \sqrt{2\Omega_{ij}\Omega_{ij}}, \quad \Omega_{ij} = \frac{1}{2}\left(\frac{\partial \overline{u_i^{\text{inc}}}}{\partial x_j} - \frac{\partial \overline{u_j^{\text{inc}}}}{\partial x_i} \right). \tag{16}$$

$\zeta - f$ **based DDES model**   The $\zeta - f$ model was described in [5] and the equations are given as

$$\frac{\partial k}{\partial t} + \overline{u_j^{\text{inc}}} \frac{\partial k}{\partial x_j} = P_k + \frac{\partial}{\partial x_j}\left[\left(\nu + \frac{\nu_t}{\sigma_k} \right) \frac{\partial k}{\partial x_j} \right] - \varepsilon, \tag{17}$$

$$\frac{\partial \varepsilon}{\partial t} + \overline{u_j^{\text{inc}}} \frac{\partial \varepsilon}{\partial x_j} = \frac{C_{\varepsilon 1} P_k - C_{\varepsilon 2} \varepsilon}{\tau} + \frac{\partial}{\partial x_j}\left[\left(\nu + \frac{\nu_t}{\sigma_k} \right) \frac{\partial \varepsilon}{\partial x_j} \right], \tag{18}$$

$$\frac{\partial \zeta}{\partial t} + \overline{u_j^{\text{inc}}} \frac{\partial \zeta}{\partial x_j} = f - \frac{\zeta}{k} P_k + \frac{\partial}{\partial x_j}\left[\left(\nu + \frac{\nu_t}{\sigma_k} \right) \frac{\partial \zeta}{\partial x_j} \right], \tag{19}$$

$$L^2 \nabla f - f = \frac{1}{\tau}\left(C_1 + C_2' \frac{P_k}{\varepsilon} \right)\left(\zeta - \frac{2}{3} \right), \tag{20}$$

where ε is the dissipation, f is the elliptic relaxation term, L is the length scale and τ is the time scale of turbulence. A detailed description of the equations and the value of the coefficients can be found in [5].

The delayed detached-eddy simulation (DDES) model modifies URANS models to achieve an LES content, enabling the DDES model to switch between URANS and LES according to the numerical resolution [16]. For the $\zeta - f$ model, the ε in the k equation is modified to

$$\varepsilon = \frac{k^{3/2}}{l_{\text{turb}}}, \tag{21}$$

where l_{turb} is the length scale of DDES

$$l_{\text{turb}} = l_{\text{RANS}} - f_d \max(0, d - C_{\text{DES}}\Delta\phi). \tag{22}$$

The turbulent viscosity is then calculated using

$$\nu_t = C_\mu \zeta k \tau. \tag{23}$$

Large eddy simulation   For LES, τ_{ij} in (10) is called the sub-grid scale stress, which is commonly modeled using the Smagorinsky model [14]

$$\tau_{ij}^{\text{Smag}} - \frac{1}{3}\tau_{kk}\delta_{ij} = -2\nu_t\overline{S_{ij}}, \quad \nu_t = (C_s\Delta)^2|\overline{S}|, \tag{24}$$

where $|\overline{S}|$ is the magnitude of the strain rate tensor, which is represented by

$$\overline{S_{ij}} = \frac{1}{2}\left(\frac{\partial \overline{u_i^{\text{inc}}}}{\partial x_j} + \frac{\partial \overline{u_j^{\text{inc}}}}{\partial x_i}\right). \tag{25}$$

3   NUMERICAL REALIZATION

This research is conducted within an in-house code FASTEST, which adopts a fully conservative finite-volume method to solve the incompressible NSE on a block-structured grid. The work flow of the aeroacoustic simulation is shown in Fig.1.
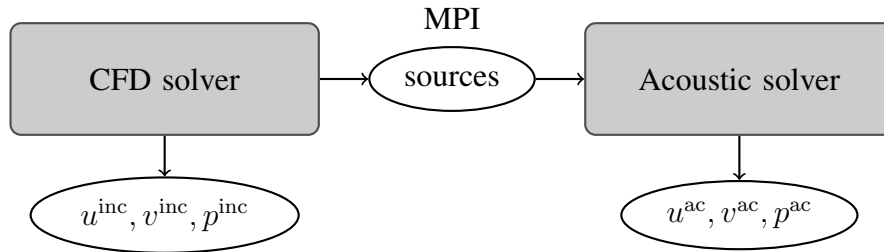

Figure 1: Numerical realization of flow solver and acoustic solver.

First, we use the different turbulence models to calculate the acoustic sources on a flow grid, which has a fine resolution. Second, we transmit and interpolate the acoustic sources onto an acoustic grid, which has a relatively coarse resolution. For the coupling of the two grids, trilinear interpolation is used owing to the simplicity of implementation. Finally, we compute the acoustic quantities by solving the LEE.

The linearized Euler equations are solved using a high-resolution scheme, which combines the first order Godunov method and the second order Lax-Wendroff method [7]. Since the flow and the acoustic variables have different time scales, the flow and the acoustic field are not computed using the same time step. Instead, each time step of the flow is further divided into several time steps for the acoustic computation.

4   TEST CASE

The main objective of this paper is to study the aeroacoustic performance of different turbulence models. For this purpose, the aeroacoustic experimental data of Etkin et al. [3] are used to compare different turbulence models. This test case investigates the flow past a cylinder and the acoustic quantities generated by the turbulent flow. The inlet flow velocity is 68.6 m/s, implying a Mach number of Ma=0.2 such that the incompressibility assumption is reasonable. The diameter of the cylinder is D=0.0125m. The Reynolds number is approximately 60000, indicating that the flow is fully turbulent.

As can be seen in Fig.2, the domain has a length of 22D in x-direction and 10D in y-direction. In order to capture the three dimensional turbulent features, the z-direction is modeled with a length of 4D.
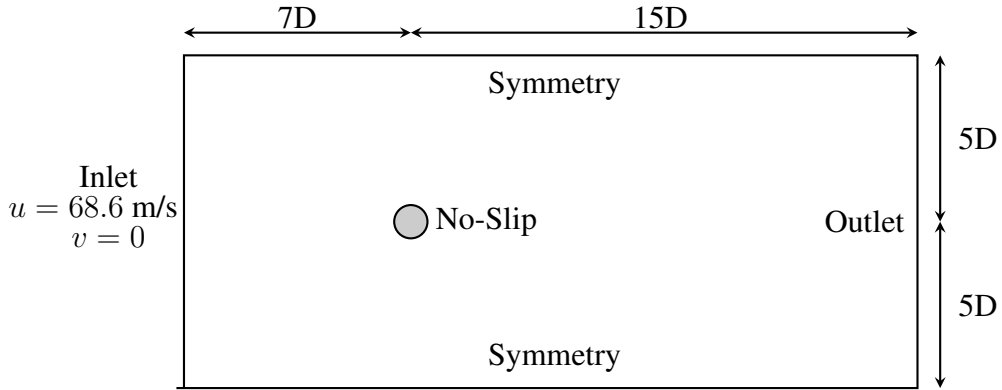
Figure 2: Sketch and boundary conditions of flow domain.

The problem domain is discretized using a block-structured grid. Figure 3a shows the spatial discretization of the flow domain. The flow is resolved up to the boundary layer, resulting in the dimensionless wall distance $y^+ < 1$. Figure 3b illustrates the discretization of the acoustic domain. Considering that the experimental data are collected at a distance of 48D from the cylinder's center, the acoustic domain has a length of 100D in each direction.
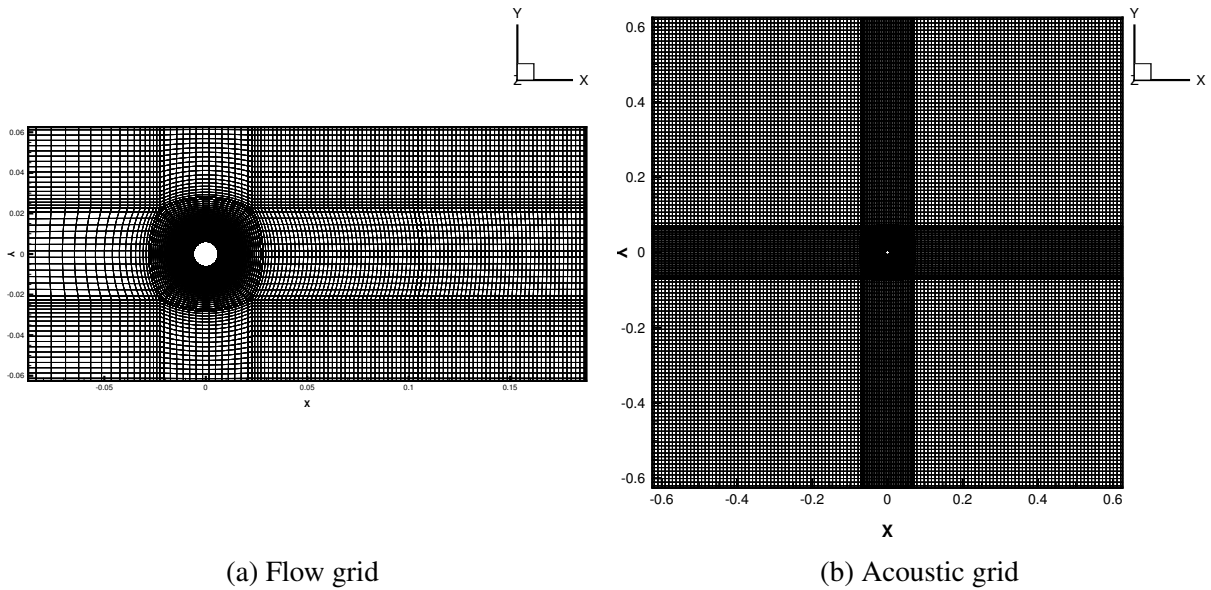

(a) Flow grid

(b) Acoustic grid

Figure 3: Discretization of flow domain and acoustic domain

The number of CVs for the flow and acoustic domains are listed in Table 1. In the LES model, 80% of the turbulence energy should be resolved. Hence, it needs a relatively fine grid to achieve adequate simulation results. A flow grid with about 2.5 million cells is adopted in this work. For the URANS model, a relatively coarse grid is utilized. The grid for the DDES model is created according to the grid resolution requirements from [17]. Regarding the time discretization, the second order fully implicit scheme is adopted, which has no stability problem when the CFL number is greater than 1 [11]. In order to fairly compare the SPL spectrum of different models, the sampling frequency is kept the same, which is realized by setting the time step for the flow to 3×10^{-6}s for all cases.
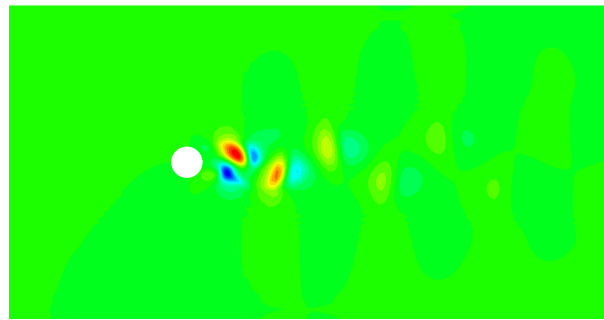
Table 1: Turbulence models and number of CVs.

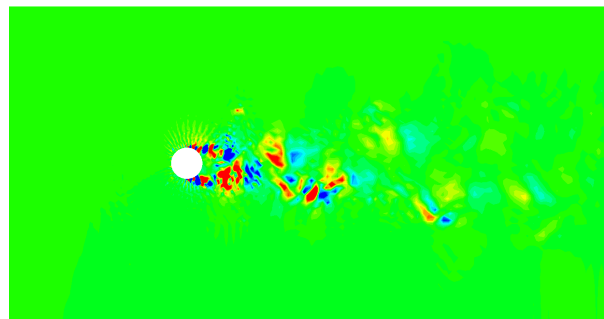| Simulation	Turbulence model	No. of CVs of flow domain	No. of CVs of acoustic domain
No.1	LES	2500368	158496
No.2	$\zeta - f$ based DDES	1233648	158496
No.3	$k - \omega$ SST	184480	158496

5 RESULTS AND DISCUSSION
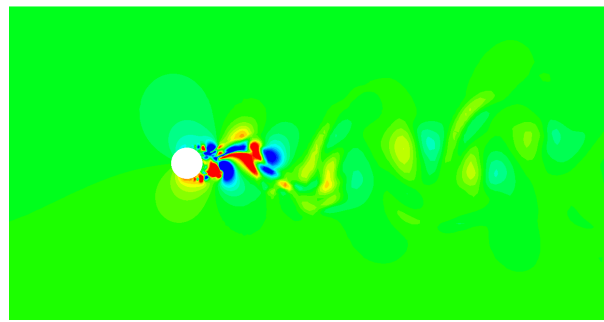
(a) Acoustic source of LES model in [Pa/s]

(b) Acoustic source of URANS model in [Pa/s]

(c) Acoustic source of DDES model in [Pa/s]

Figure 4: Acoustic sources obtained by different turbulence models

In order to acquire a fully developed von Kármán vortex street and a stable propagation process of acoustics, 30000 time steps are observed. For the calculation of this time period, the LES model requires approximately 4 days, the DDES model needs 2.5 days, while the URANS model needs only 10 hours.

Figure 4 shows the acoustic sources predicted by three different turbulence models. According to the simulation of LES, as shown in Fig.4a, the acoustic sources appear predominantly in the wake region and the shear layer. The URANS model is not suitable to predict the acoustic source in the shear layer, as indicated in Fig.4b. In the wake region, only large periodic sources can be predicted to some extent. Figure 4c illustrates that the DDES turbulence model can predict the acoustic sources in the shear layer accurately. However, the acoustic sources in the wake region can only be partially predicted. This may be caused by the "grey area" problem. The DDES model switches between LES and RANS modes depending on the numerical resolution. However, there often exist regions where it is neither LES nor RANS mode, resulting in a large simulation error in such areas. This problem can emerge after the flow separation, where the mode should be changed from RANS to LES. Due to the insufficient turbulence information from the RANS mode from the upstream, the LES mode can not develop immediately after the transition.

As in the experiment of Etkin et al. [3], the acoustic data at an observer point are collected, which is placed at a distance of 48D from the cylinder's center perpendicular to the flow direction. The $1/3$ octave spectrum of the simulations and the experimental data are given in Fig.5.
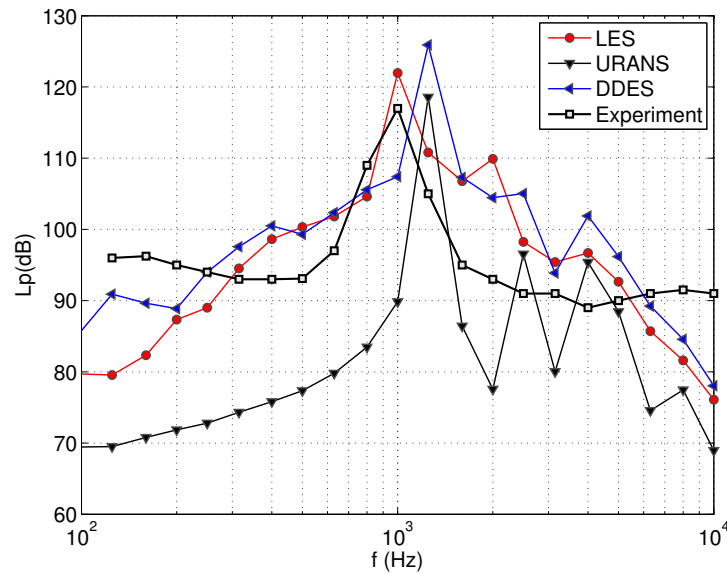

Figure 5: Comparison of SPL of different turbulence models with experimental data

The LES model offers the closest comparison with the experimental data. The underprediction in the high frequency region is caused by the filtering process in LES, which leads to a loss of the high frequency fluctuation component in the flow. In addition, as shown in Table 2, the fundamental frequency obtained by LES is 1061Hz, which has a relative error of only 6.1%. As illustrated in Fig.5, the SPL of the $k - \omega$ SST model has an obvious deviation from the experimental data. Nevertheless, this URANS model can provide the fundamental frequency with a relative error of 22%.

For the $\zeta - f$ based DDES model, a similar SPL spectrum to the LES model is observed.

However, it can only predict the fundamental frequency with a similar accuracy as the URANS model, as indicated in Table 2.

Table 2: Fundamental frequency.

	Frequency (Hz)	Error
Experiment	1000	-
LES	1061	6.1%
URANS ($k - \omega$ SST)	1222	22%
$\zeta - f$ based DDES	1200	20%

6   CONCLUSION

Three different turbulence models have been investigated in the context of aeroacoustic simulation. The SPL spectrum of the LES model shows the best agreement with the experimental data. The underprediction in the high frequency region is also reasonable. The URANS model can only provide the fundamental frequency with a modest error. Its SPL spectrum deviates obviously from the experimental data. In comparison to URANS, the DDES model has been shown to be able to predict the SPL spectrum with a satisfactory accuracy. However, only a minimal improvement in predicting the fundamental frequency is observed.

7   ACKNOWLEDGMENT

REFERENCES

[1] C. Bailly, C. Bogey, O. Marsden, Progress in direct noise computation. *International Journal of Aeroacoustics*. 9(1):123-143, 2010.,

[2] N. Curle, The influence of solid boundaries upon aerodynamic sound, *Proceedings of the Royal Society (London)*. 231(A):505-514, 1955.

[3] B. Etkin, G.K. Korbacher, R.T. Keefe, Acoustic Radiation from a Stationary Cylinder in a Fluid Stream (Aeolian Tones). *Journal of the Acoustical Society of America*. 2930-36, 1957.

[4] J. Fröhlich, D. Terzi, Hybrid LES/RANS methods for the simulation of turbulent flows, *Progress in Aerospace Sciences*, 44(2008):349-377, 2008.

[5] K. Hanjalić, M. Popovac, M. Hadžiabdić, A robust near-wall elliptic-relaxation eddy-viscosity turbulence model for CFD. *International Journal of Heat and Fluid Flow*, 25(6):1047-1051, 2004.

[6] J.C. Hardin, D.S. Pope, An acoustic/viscous splitting technique for computational aeroacoustics. *Theoretical and Computational Fluid Dynamics*. 6(5):323-340, 1994.

[7] M. Kornhaas, M. Schäfer, D.C. Sternel. Efficient numerical simulation of aeroacoustics for low Mach number flows interacting with structures. *Computational Mechanics*, 55:1143-1154, 2015.

[8] M.J. Lighthill, On Sound Generated Aerodynamically. I. General Theory. *Proceedings of The Royal Society of London A*. 211:564-587, 1952.

[9] M.J. Lighthill, On Sound Generated Aerodynamically. II. Turbulence as a source of sound. *Proceedings of The Royal Society of London A*.Volume 222, pp. 1-34, 1954.

[10] F.R. Menter, Two-Equation Eddy-Viscosity Turbulence Models for Engineering Applications *AIAA Journal*, 32(8):1598-1605, 1994.

[11] M. Schäfer, *Computational Engineering - Introduction to Numerical Methods*. Springer, 2006.

[12] W.Z. Shen, J.N. Sørensen, Aeroacoustic Modelling of Low-Speed Flows *Theoretical and Computational Fluid Dynamics*. Volume 13, Issue 4, pp. 271-289, 1999.

[13] W.Z. Shen, J.N. Sørensen, Comment on the aeroacoustic formulation of Hardin and Pope. *AIAA Journal*. 37(1):141-143, 1999.

[14] J. Smagorinsky, General circulation experiments with the primitive equations I: The basic experiment *Monthly weather review*, 91(3):99-163, 1963.

[15] P.R. Spalart. Detached-eddy simulation. *Annual Review of Fluid Mechanics*, 41(1):181-202, 2009.

[16] P.R. Spalart, S. Deck, M.L. Shur, K.D. Squires, M.Kh Strelets, A. Travin. A new version of detached-eddy simulation, resistant to ambiguous grid densities. *Theoretical and Computational Fluid Dynamics*, 20(3):181-195, 2006.

[17] P.G. Tucker, Unsteady Computational Fluid Dynamics in Aeronautics, *Fluid Mechanics and Its Applications*, Volume 104, 2014.